Journal of Materials Chemistry A

PAPER

View Article Online
View Journal

Cite this: DOI: 10.1039/c7ta00527j

Full-cell quinone/hydroquinone supercapacitors based on partially reduced graphite oxide and lignin/PEDOT electrodes†

Adriana M. Navarro-Suárez,[a] Nerea Casado,[b] Javier Carretero-González,‡*[a] David Mecerreyes[b] and Teófilo Rojo*[ac]

Received 16th January 2017
Accepted 17th March 2017

DOI: 10.1039/c7ta00527j

rsc.li/materials-a

The development of new, scalable and inexpensive materials for low-cost and sustainable energy storage devices is intensely pursued. The combination of redox active biopolymers with electron conducting polymers has shown enhanced charge storage properties. However, their performance has just been investigated at the electrode level. Herein, we move a step further by assembling full-cell supercapacitors based on natural lignin (Lig) and partially reduced graphite oxide (prGrO) electrode materials. Both materials evidenced that quinone/hydroquinone redox moieties are able to store and release charge reversibly. The redox properties of lignin were improved by combining it with poly(3,4-ethylenedioxythiophene) (PEDOT). Analysis of the capacitive contributions to the charge storage proved that PEDOT enhanced the lignin's capacitive contribution to the current by 22%. The capacitive contributions were equal to 66% and 75% in Lig/PEDOT blend and prGrO electrodes, respectively. We also show for the first time that by distributing equally charges in carbon–biopolymer composite electrodes, a higher capacitance retention, up to 79% after 1000 cycles, is achieved.

Introduction

Pushing forward the development of sustainable technology for energy storage requires the choice of low-cost and earth abundant materials working as electrodes in electrochemical cells. Redox active polymers are well positioned for the development of high-energy density electrode materials in batteries and supercapacitors because of their high flexibility for tuning the redox voltage and capacitance.[1–3] In addition, they are easily processable and recyclable as well as environmentally friendly (metal-free). Although there are a large number of suitable polymeric compounds for the storage of charge[4–6] those containing quinones have received great attention, since they have high theoretical capacity, high electron transfer kinetics, and excellent redox reversibility and are of low cost.[7,8]

Redox active phenol and quinone compounds are found in plants and wood. Actually, black liquor, a by-product of cellulosic paper processing, contains lignins rich in phenol groups which can be further converted to quinones through electrochemical oxidation processes.[9] In a pioneering study, Inganäs and Milczarek showed charge storage on lignin sulfonate–polypyrrole thin film electrodes in an aqueous based electrolyte.[10] In this scientific work, the biopolymer was combined with the conducting polymer polypyrrole (PPy). The conducting polymer facilitated the transport of electrons and ions from the electrolyte to the lignin moiety. In addition, various combinations of lignin and other electron conductors[11–16] such as reduced graphene oxide[17] or carbon nanotubes[18] have been investigated as electrode materials. More recently, poly(3,4-ethylenedioxythiophene) (PEDOT) was used to facilitate the electron transfer in Lig/PEDOT electrodes for supercapacitor applications. Electrodes based on Lig/PEDOT showed an excellent capacitance retention (83% after 2000 cycles). This was much higher than that in the case of a lignin/polypyrrole blend where strong degradation after cycling was observed.[19] However, lignin has not been tested in a full-cell configuration yet, as previous studies have focused on its electrochemical characterization as an electrode material.

Herein, we moved a step further by assembling two different full cell supercapacitors containing both partially reduced graphite oxide (prGrO)[20] containing a majority of quinone groups[21] and a Lig/PEDOT biopolymer as electrodes. In the first assembly, prGrO and Lig/PEDOT are used in an asymmetric device as negative and positive electrodes, respectively. In the second one, a composite of both materials is prepared and tested in a symmetric configuration. Different peak potentials are evidenced for both Lig/PEDOT and prGrO electrodes as the

[a]CIC EnergiGUNE, Albert Einstein 48, 01510 Miñano, Alava, Spain. E-mail: trojo@cicenergigune.com

[b]POLYMAT, University of the Basque Country UPV/EHU, Joxe Mari Korta Centre, Avda. Tolosa 72, 20018, Donostia-San Sebastian, Spain

[c]Inorganic Chemistry Department, University of the Basque Country, P. O. Box 644, 48080 Bilbao, Spain

† Electronic supplementary information (ESI) available. See DOI: 10.1039/c7ta00527j

‡ Current address: Institute of Polymer Science and Technology, CSIC, Juan de la Cierva 3, 28006, Madrid, Spain, jabenzo@hotmail.com.

electrochemistry of quinone functionalities is determined by their chemical neighbors.[22] Multiple redox states are also achieved by combining both materials in a single electrode; so excellent cell capacitance values up to 36 F g^{-1} are evidenced. Interestingly, these capacitance values observed for a full device are higher than the ones observed in symmetric cells of each material separately.

Experimental

Lignin/PEDOT polymerization

Natural lignin is isolated following a process explained elsewhere.[23] Lignin/PEDOT polymers are synthesized *via* chemical oxidative polymerization of the EDOT monomer in the presence of lignin, by using iron(III) chloride as the catalyst and sodium persulfate as the primary oxidant at room temperature for 8 hours, as explained elsewhere.[19] In this case, as lignin is not sulfonated, the mixture containing lignin and the oxidant is stirred in water for 8 hours in order to partially solubilize the lignin. Then, the EDOT monomer is added and the mixture is stirred at room temperature for 8 more hours. Finally, lignin/PEDOT dispersions are dialyzed with deionized water using 12 000–14 000 Da molecular weight cut-off membranes for 2 days. After freeze-drying, the Lig/PEDOT polymers are obtained as a dark bluish powder. The initial lignin : EDOT mass ratios used are 0 : 100, 20 : 80, 40 : 60 and 60 : 40 yielding the as-called PEDOT, Lig/PEDOT 20/80, Lig/PEDOT 40/60 and Lig/PEDOT 60/40 polymers, respectively. In order to confirm the polymerization between lignin and EDOT, Fourier transform infrared (FTIR) spectroscopy and thermogravimetric analyses (TGA) are performed on the lignin and the Lig/PEDOT polymers.

Partially reduced graphite oxide synthesis

Graphite powder (Sigma Aldrich, particle size < 20 μm, cat#282863) is oxidized by the Marcano–Tour method, described elsewhere.[20] Briefly, a 9 : 1 mixture of concentrated sulfuric and phosphoric acids (H_2SO_4/H_3PO_4, 360 : 40 mL) is added to a mixture of graphite powder (3.0 g, 1 wt equiv.) and potassium permanganate ($KMnO_4$, 18.0 g, 6 wt equiv.). The reaction mixture is then heated to 50 °C and stirred overnight. The reaction mixture is cooled to room temperature and poured onto ice (~400 mL) with 30% hydrogen peroxide (H_2O_2, 3 mL). The solution is centrifuged (10 000 rpm for 30 min), and the supernatant is decanted away. The remaining solid material is then washed in succession with 200 mL of water, 200 mL of 30% hydrochloric acid (HCl), and then with water until neutral pH; for each wash, the mixture is centrifuged (10 000 rpm for 30 min) and the supernatant is decanted away. The solid obtained is vacuum-dried overnight at 60 °C. Graphite oxide (GrO) is then heated, under an argon flow, at a heating rate of 5 °C min^{-1} up to 160 °C, followed by an isothermal step of 1 hour. The solid obtained is referred to as prGrO (partially reduced graphite oxide).

Fourier transform infrared

Fourier transform infrared spectra are acquired at room temperature using a Thermo Scientific Model Nicolet 6700 FT-IR spectrometer, applying 10 scans in transmission mode using KBr pellets.

Thermogravimetric analyses

Thermogravimetric analyses are performed on a TGA Q500 (TA Instruments). Measurements are carried out by heating around 3 mg of the sample at 10 °C min^{-1} under a nitrogen atmosphere from room temperature to 800 °C.

X-ray photoelectron spectra (XPS)

X-ray Photoelectron Spectra (XPS) are recorded on a KRATOS AXIC 165 equipped with Mg Kα radiation and a hemispherical analyzer Phoibos 150 with a 3D-DLD detector (SPECS). The binding energy (BE) of all the samples is tested as referenced to C 1s at 284.8 eV. The assignment of C 1s and O 1s components is based on theoretical predictions of core level shifts and on reported spectra containing the particular oxygen functional groups.[24,25] The XPS peaks are fitted to pseudo-Voigt functions having 80% Gaussian and 20% Lorentzian characters, after performing a Shirley background subtraction.

Electrochemical characterization

In the cavity microelectrode (CME) the electrochemical interface area is around a fraction of mm^2 and the ohmic drop coming from the bulk of the electrolyte can be neglected, allowing the use of high scan rates.[26] Lignin, Lig/PEDOT 40/60 and prGrO are tested electrochemically in a 3-electrode configuration with a microcavity as the working electrode, a platinum wire as the counter electrode, a silver/silver chloride (Ag/AgCl) electrode as the reference electrode in a 0.1 M perchloric acid ($HClO_4$) electrolyte solution. The microcavity is filled with the active material by pressure of the carbon powders against a glass plate. The cavity is cleaned by immersing the electrode in ethanol in an ultrasonic bath between experiments. Because the quantity of material inserted in a cavity micro-electrode is unknown, Swagelok cells were assembled to quantify the capacitance achieved by the electrode materials in a 0.1 M $HClO_4$ electrolyte solution. For the tests carried out by using a 3-electrode cell, a Ag/AgCl electrode is used as the reference electrode and a platinum mesh is used as the counter electrode. The symmetric and asymmetric cells are electrochemically studied by using a Ag/AgCl electrode as the reference electrode. Electrochemical cyclic voltammetry (CV) measurements at different scan rates ranging from 1 to 40 mV s^{-1} as well as rate capability measurements in galvanostatic mode at different current densities ranging from 0.1 to 10 A g^{-1} are performed under ambient conditions in a multichannel potentiostat/galvanostat (Biologic VMP3, France). Capacitance values per electrode are usually reported, which are valid for symmetric cells and 3-electrode characterization. However, for asymmetric devices, these values are not accurate enough as each electrode has a different mass. In this article, we will refer to capacitance when the electrode capacitance was calculated and to cell capacitance when both electrode masses were used. Cell capacitance is calculated using eqn (1):

$$C_{\text{cell}} = i/((\mathrm{d}v/\mathrm{d}t) \times (m_+ + m_-)) \quad (1)$$

where C_{cell} is the cell capacitance, i is the measured current, dv/dt is the scan rate, and m_+ and m_- correspond to the mass of the positive and negative electrodes, respectively.[27]

Electrode preparation

The lignin/PEDOT and lignin/PEDOT//prGrO electrodes are drop-cast on a platinum mesh from an aqueous solution. The electrodes are left to dry at room temperature in air for 8 h before testing. The prGrO is suspended in ethanol and filtered under vacuum by using polytetrafluoroethylene membranes (Sartorius, pore size 0.45 μm and 4.5 cm diameter) and dried in a vacuum oven at 60 °C for 8 h, resulting in a prGrO film that detaches easily from the membrane and can be further used as a free-standing electrode.

Results and discussion

Structural characterization of the electrode materials

In this work, partially reduced graphite oxide (prGrO) and the Lig/PEDOT polymer, both containing quinone/hydroquinone moieties (shown as green circles in Scheme 1), are investigated as electrode materials for supercapacitors. First, Lig/PEDOT was obtained *via* oxidative polymerization of EDOT in the presence of lignin as reported before.[18] Second, prGrO was synthesized by oxidation of graphite powder by the Marcano–Tour method.[19] The obtained graphite oxide (GrO) is later heated under an argon flow to produce the desired prGrO electrode material.[18]

The synthetic route allows preparing Lig/PEDOT polymers with different compositions of each component. In this work, we investigated several compositions of which the one with 40 wt% lignin and 60 wt% PEDOT shows the optimum electrochemical properties (discussed in the next section). The chemical properties of Lig/PEDOT electrode materials are studied using Fourier transform infrared spectroscopy (FTIR) measurements (Fig. S1a†). All the Lig/PEDOT polymers exhibit vibration bands related to lignin and PEDOT structures and the intensity of the bands varies depending on the composition of the polymer.[19] All the polymers are thermally stable up to 190 °C as observed in the thermogravimetric analysis (TGA) (Fig. S1b†).[23,28]

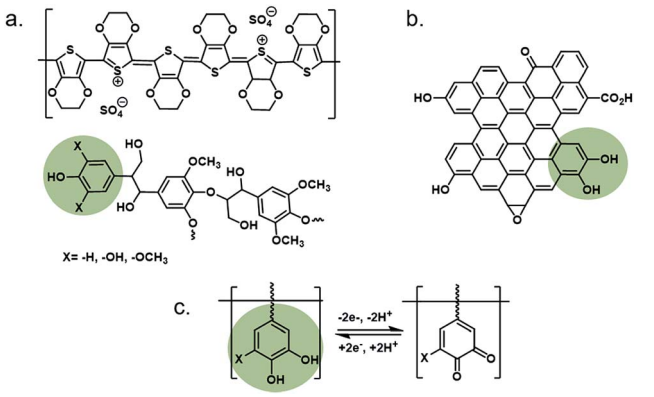

Scheme 1 Structure of electrode materials used in this work: Lig/PEDOT (a) and partially reduced graphite oxide, prGrO (b). Quinone/hydroquinone redox reaction (c).

Using the Marcano–Tour method, the partially reduced graphite oxide (prGrO) was analyzed by X-ray Photoelectron Spectroscopy (XPS) (Fig. S2†) and Fourier transform infrared spectroscopy (FTIR) (Fig. S3†). The comparison of the C 1s XPS spectra of GrO and prGrO confirms the partial restoration of the C=C bonds. The O 1s spectra (Fig. S2b†) reinforce this information, and the increase of C–O bonds suggests the formation of phenol (or aromatic diol) groups during deoxygenation due to the close proximity of C–OC and C–OH on the basal plane.[29] The chemical changes from GrO to prGrO are also determined by Fourier transform IR spectroscopy (Fig. S3†). The decrease in the C=O bonds, when comparing prGrO with GrO, and the increase in all the other bonds agree with the results from XPS and reinforce the hypothesis of phenol and/or aromatic diols as the main functional groups in the prGrO. The presence of a majority of quinone groups in this kind of graphite oxide was already reported by Eng *et al.*, who noticed that quinone/hydroquinone functionalities are the likely source of the redox reactions observed in graphene oxide prepared by the Marcano–Tour method.[21] Eng *et al.* showed that this kind of GrO presents a dominant peak assigned to C–O groups with a C/O ratio of around 1.9 caused by the high degree of oxidation. Based on these quinone/hydroquinone functionalities and on their different peak potentials, Lig/PEDOT and prGrO were characterized electrochemically for use as electrodes in full-cell supercapacitors.

Electrochemical characterization of the electrode materials

First, we determined the capacitive contributions of both materials to the current. For this purpose, initial voltammetric measurements were made in a cavity micro-electrode (CME). Two separate mechanisms, surface capacitive effects and diffusion-controlled processes, can be discriminated by relating the current response to the voltammetric sweep rate according to the following equation:[27]

$$i/v^{1/2} = k_1 v^{1/2} + k_2 \quad (2)$$

where i is the measured current, v is the sweep rate, and k_1 and k_2 are related to the current contributions from the surface capacitive effects and the diffusion-controlled intercalation process, respectively. Fig. S4† and 1 show the cyclic voltammetry curves of lignin, Lig/PEDOT 40/60 and prGrO at 100 mV s^{-1}. By plotting $i/v^{1/2}$ *vs.* $v^{1/2}$, according to eqn (2), the values of k_1 and k_2 are calculated in the whole potential window and therefore we are able to quantify the fraction of the current due to each of these contributions.

The comparison between Fig. S4† and 1a shows us noticeable differences in the electrochemical properties between lignin and Lig/PEDOT polymer materials. In Fig. S4,† the lignin–CNT material presents a narrow peak corresponding to the redox process of the quinone groups present in lignin.[10] This peak is present in both curves proving that this reaction occurs both on the surface of the material (pseudocapacitive process) and in the bulk electrode material. The total capacitive contribution is 42% at 100 mV s^{-1}.

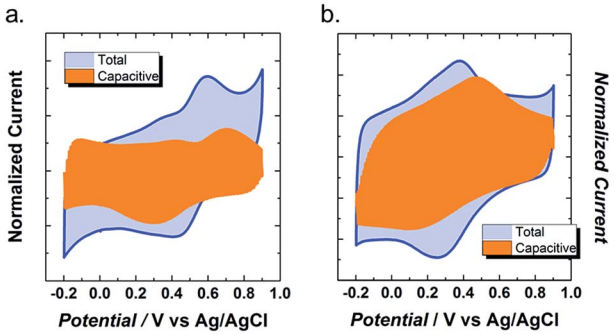

Fig. 1 Total (blue area) and capacitive contributions (orange area) of Lig/PEDOT 40/60 (a) and prGrO (b) to the electrochemical charge storage in 0.1 M $HClO_4$.

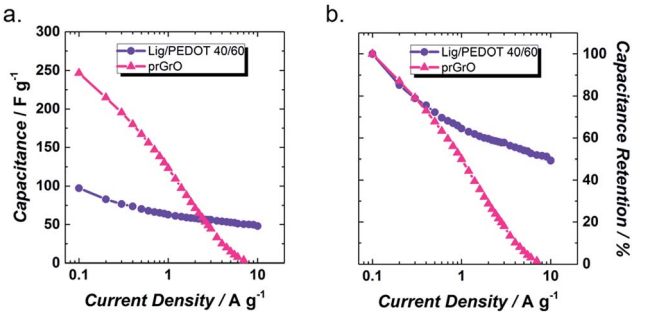

Fig. 2 Rate capability (a) and capacitance retention (b) of the Lig/PEDOT 40/60 and the prGrO in 0.1 M $HClO_4$.

The electrochemistry of the Lig/PEDOT changes dramatically (Fig. 1a) when compared to the lignin one (Fig. S4†). First, the potential window increases by 0.20 V, going from −0.2 V to 0.9 V *vs.* Ag/AgCl, indicating that PEDOT stabilizes the electrochemical processes occurring in the lignin in this electrolyte. Second, the peaks attributed to the quinone/hydroquinone redox pair (Scheme 1c) in lignin–CNT are now broader and more separated, indicating a more heterogeneous distribution of charged species across the electrode material. Third, the shape of the cyclic voltammetric curve is more rectangular indicating a remarkable capacitive process compared to the lignin–CNT composite. These two last points are confirmed by the increase of the capacitive contribution up to 66% at 100 mV s^{-1}. These results prove that PEDOT is an adequate facilitator for transferring electrons to the lignin and the Lig/PEDOT polymer is ideal for supercapacitor applications thanks to the retention of its capacitive contribution at high scan rates.

Similar to lignin, the prGrO material (Fig. 1b) also shows redox peaks corresponding to the redox reactions involving the quinone/hydroquinone moieties (Scheme 1b). In this case, the potential at which these processes occur is below 0.6 V, because of the different neighboring chemical structure than that of lignin. The presence of these functional groups was confirmed by XPS and FTIR experiments. The capacitive charge storage corresponds to 75% of the total current at 100 mV s^{-1} and is caused by double-layer and pseudocapacitive processes. Most of this capacitance might be caused either by redox pseudocapacitance involving again the quinone/hydroquinone functionalities (Scheme 1b) or intercalation pseudocapacitance.

Fig. 2 and S5† show the rate capability and capacitance retention of the different Lig/PEDOT biopolymers and the prGrO electrodes by using 0.1 M $HClO_4$ as the electrolyte in a 3-electrode configuration. The electrochemical properties of the biopolymer electrodes were influenced by the Lig/PEDOT ratio. The highest capacitance value, 97 F g^{-1}, is achieved by Lig/PEDOT 40/60 at 0.1 A g^{-1}, with 51% of this capacitance retained at 10 A g^{-1}. Ajjan *et al.* have found higher capacitance values for their Lig/PEDOT biocomposites; however, these results correspond to EDOT electropolymerized in the presence of commercial ligninsulfonate.[19] Differences in the amount of quinone units in between the commercial lignin and the one derived from the black liquor might be the cause for differences in the capacitance values. The quinone groups in the prGrO should also yield high capacitance values, because these redox reactions arise from both the surface and the bulk material. However, a depletion of the quinone group with increase of the current density or cycling is also expected.[30] Fig. 2 shows the rate capability of the prGrO film, which achieves capacitance values up to 248 F g^{-1}, but is diminished, rapidly with increasing of the current density.

Electrochemical characterization of full-cell supercapacitors

An asymmetric full-cell based on Lig/PEDOT 40/60 as the positive electrode and prGrO as the negative electrode was assembled (Fig. 3a). This device will take advantage of the redox reactions occurring above 0.6 V *vs.* Ag/AgCl in the Lig/PEDOT polymer and its high capacitance retention as well as the large capacitance values exhibited by the prGrO electrode caused by the redox reactions occurring below 0.6 V *vs.* Ag/AgCl.

By principle, the charge (q) stored at the positive and negative electrodes is equivalent ($q_+ = q_-$). This charge depends on the specific capacitance (C), the potential window (ΔE) and the mass (m) of each electrode following the equation below:[31]

$$q = C \times \Delta E \times m \quad (3)$$

Assuming that both electrodes have the same potential window, their masses are balanced based on their capacitance values at 0.1 A g^{-1}, as follows:

$$C_+ \times m_+ = C_- \times m_- \quad (4)$$

$$m_+/m_- = C_-/C_+ = 248/97 = 2.6 \quad (5)$$

For comparison, symmetric cells of each material are assembled and their main electrochemical results are shown in Fig. S6.† Fig. 3b–g show the electrochemical characterization of the asymmetric Lig/PEDOT//prGrO device with $m_+/m_- = 2.6$. For comparison of the symmetric and asymmetric devices, the cell capacitance values are henceforth reported. The CVs of the asymmetric device in Fig. 3b show that despite having two diffusion-limited processes, the total effect is an almost rectangular CV, similar to the ones exhibited by double-layer capacitors. This behavior is maintained at different scan rates,

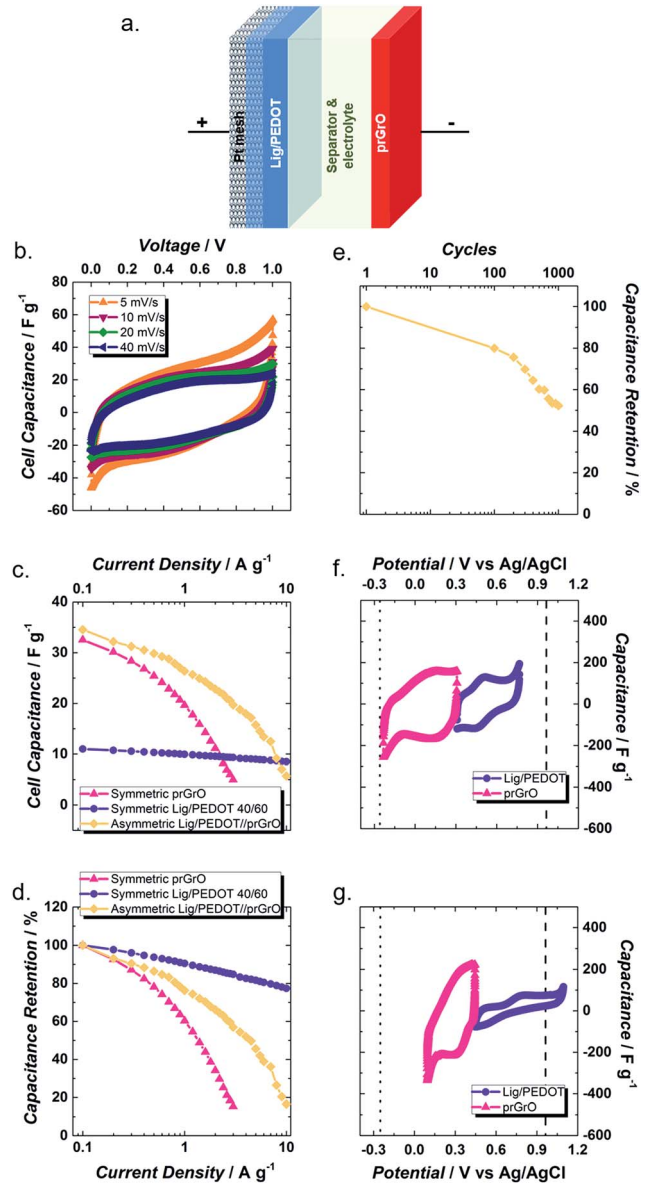

Fig. 3 Schematic diagram structure (a) and electrochemistry of the asymmetric Lig/PEDOT//prGrO device in 0.1 M $HClO_4$ electrolyte. Cyclic voltammetry (b), rate capability (c), capacitance retention (d), capacitance retention during the 1000-cycle test at 5 mV s^{-1} (e), 2nd cycle CV (f) and 1000th cycle CV (g). Dashed and dotted lines in (f) and (g) denote the water stability window.

demonstrating acceptable electron conductivity. By using an asymmetric device, the capacitance is increased to 34.6 F g^{-1}, 7% and 69% higher than that of the symmetric cells of prGrO and Lig/PEDOT 40/60 (Fig. 3c), respectively. Fig. 3d shows that at 10 A g^{-1}, the asymmetric device still maintains 17% of its initial capacitance. These effects, large capacitance and intermediate capacitance retention, are caused by a synergistic effect between Lig/PEDOT and prGrO materials. The former provides capacitance retention while the latter delivers high capacitance values.

The asymmetric Lig/PEDOT//prGrO device was cycled at 5 mV s^{-1} 1000 times. Fig. 3e shows the capacitance retention of the device every 100 cycles. The results show that the device maintains 52.2% of its initial capacitance after 1000 cycles. In order to understand the reason for this loss of capacitance, a pseudo-reference electrode is introduced to study the electrochemical processes in each electrode. Cycle numbers 2 and 1000 of each electrode are shown as examples; as the capacitance values are reported per electrode the performance of the full device is omitted in this figure. Fig. 3f shows the 2nd cycle of the cycle life measurement of the asymmetric device. The positive electrode, Lig/PEDOT 40/60, shows the redox peaks, characteristic of the quinone/hydroquinone process (Scheme 1c). The negative electrode, prGrO, presents wider peaks, most probably due to pseudocapacitive processes. The potential windows are 0.46 V and 0.54 V for the positive and negative electrodes, respectively, showing that the initial mass balance is appropriate for this full-cell device. The device is electrochemically cycled first towards positive voltages, which oxidizes the hydroquinone groups in the Lig/PEDOT electrode while the reduction reaction occurs in the prGrO electrode. After 1000 cycles (Fig. 3g), the positive electrode expands its voltage window beyond 0.65 V, leaving the negative electrode working up to 0.35 V. This effect is caused by the decrease in capacitance in the Lig/PEDOT electrode, which might be induced by depletion of quinone groups in the material.[32] This is associated with decreased intensity of the redox peaks in the CV curve of the positive electrode as well as an increase in the polarization. At this pH, oxygen evolution theoretically takes place at 0.96 V *vs.* Ag/AgCl, which is a potential value achieved by the positive electrode and that could also be affecting the stability of the full-cell and therefore its capacitance retention after several cycles. Because of the overpotential of the water splitting reaction, the oxygen evolution at the positive electrode seems to start above 1.05 V *vs.* Ag/AgCl.

Then, we applied another strategy to further improve the electrochemical properties of the full-cell. In order to maximize the capacitance values and capacitance retention, Lig/PEDOT 40/60 and prGrO were combined into a composite electrode material; in this way the capacitive and faradaic processes would be distributed homogeneously in both electrodes. For that, both Lig/PEDOT 40/60 and prGrO materials were dissolved in water, in a 50/50 wt% ratio, and then drop-cast on a platinum mesh, which acts as the current collector (Fig. 4a). Fig. 4b–g show the main results of the electrochemical study of the composite electrodes in a symmetric cell configuration. Interestingly, the cyclic voltammetry curves of the composite electrode (Fig. 4b) are rectangular, like those of electrical double-layer capacitors. Fig. 4c shows how the distribution of charges into the electrodes might be similar because a cell capacitance value slightly higher (*i.e.* 36 F g^{-1}) than the one exhibited by the asymmetric device (34.6 F g^{-1}) was achieved. Remarkably, when the current density increases (Fig. 4d) the capacitance retention of the composite (54%) is superior to that of the asymmetric device (17%), as a result of an enhanced charge transfer in the electrodes. These devices cannot achieve the high capacitance retention of the symmetric Lig/PEDOT 40/60 cells; however, in these cases, cycle life is sacrificed for the sake of large capacitance values.

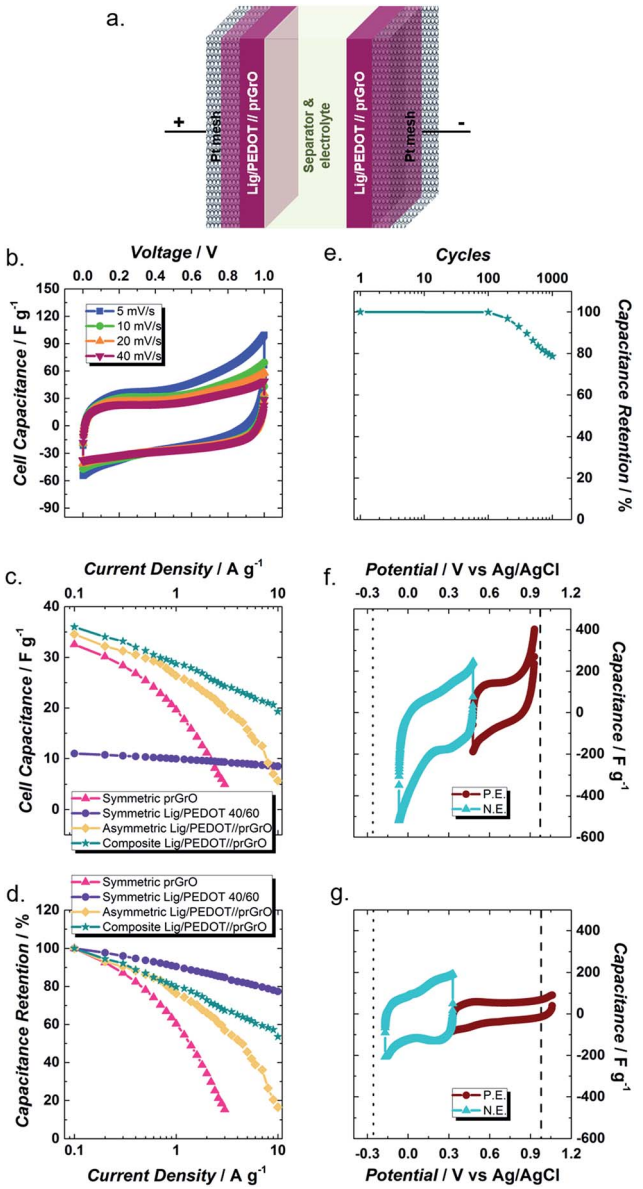

Fig. 4 Schematic diagram structure (a) and electrochemistry of the symmetric Lig/PEDOT//prGrO device in 0.1 M $HClO_4$. Cyclic voltammetry (b), rate capability (c), capacitance retention (d), capacitance retention during the 1000-cycle test at 5 mV s^{-1} (e), 2nd cycle CV (f) and 1000th cycle CV (g). Dashed and dotted lines in (f) and (g) denote the water stability window. P.E. and N.E. denote the positive and negative electrodes, respectively.

The composite cell is also tested at 5 mV s^{-1} for 1000 cycles, and the main results are shown in Fig. 4e–g. After 1000 cycles, the composite Lig/PEDOT//prGrO retains 79% of its initial capacitance (Fig. 4d). This is an important result, as the composite achieves not only higher capacitance values and higher capacitance retention but also a superior cycle life when compared to the asymmetric device. During the second cycle, the negative and positive electrodes work in a potential window of 0.55 and 0.45 V, respectively. After 1000 cycles, the new potential window is 0.40 V and 0.60 V for the negative and positive electrodes, respectively. This increase in the potential window of the positive electrode potential might be due to the depletion of the quinone groups in the positive electrode causing a decrease in its capacitance. In this configuration, the potential window of the positive electrode reaches just up to 1 V *vs.* Ag/AgCl, remaining inside the water electrochemical stability zone during all the cycles.

Conclusions

In this work, two full-cell supercapacitors were demonstrated by using a partially reduced graphite oxide (prGrO) and lignin/PEDOT as electrode materials. Asymmetric supercapacitors were assembled using Lig/PEDOT 40/60 as the positive electrode and prGrO as the negative electrode. The electrochemical results showed that the asymmetric device achieved high cell capacitance values, 34.6 F g^{-1} at 0.1 A g^{-1}, and intermediate capacitance retention when compared to symmetric cells of Lig/PEDOT 40/60 and prGrO. When cycled 1000 times at 5 mV s^{-1}, the device maintained 52.2% of its initial capacitance due to depletion of the quinone groups in the positive electrode, *i.e.* Lig/PEDOT 40/60. The use of a composite electrode prepared between the Lig/PEDOT 40/60 and the prGrO in a ratio of 50/50 improved the electrochemical properties of the full-cell. This synergistic effect might be due to the presence of a homogeneous distribution of the pseudocapacitive centers and improved electrical conductivity as a consequence of the intimate combination of both materials in the same electrode. The results confirmed the improvement by the attaining of high cell capacitance values, 36 F g^{-1} at 0.1 A g^{-1}, and a high capacitance retention, 54%, at 10 A g^{-1}. A long cycle life was also achieved by this method, maintaining 79% of its capacitance after 1000 cycles. All in all, this work demonstrated a full-cell device based on materials mostly coming from renewable sources evidencing electrochemically active quinone/hydroquinone redox moieties that are able to reversibly store and release charge.

Acknowledgements

This work was financially supported by the Graphene Flagship (Grant agreement no. 604391. Call: FP7-ICT-2013-FET-F) and European Research Council by Starting Grant Innovative Polymers for Energy Storage (iPes) 306250 (DM). AMNS (PRE_2014_1_62) and NC are supported by the Basque Government Scholarship for pre-doctoral formation. We gratefully thank Dr Oleksandr Bondarchuk for his help in the characterization measurements. Finally, the kind donation of black liquor samples by Smurfit Kappa Nervion (Basque Country, Spain) and Papelera Guipuzcoana de Zicuñaga, S. A. (Basque Country, Spain) is gratefully acknowledged.

References

1 X. Chen, H. Wang, H. Yi, X. Wang, X. Yan and Z. Guo, *J. Phys. Chem. C*, 2014, **118**, 8262–8270.
2 A. Le Comte, D. Chhin, A. Gagnon, R. Retoux, T. Brousse and D. Bélanger, *J. Mater. Chem. A*, 2015, **3**, 6146–6156.

3 N. Casado, G. Hernández, H. Sardon and D. Mecerreyes, *Prog. Polym. Sci.*, 2016, **52**, 107–135.
4 Z. Song and H. Zhou, *Energy Environ. Sci.*, 2013, **6**, 2280–2301.
5 R. Gracia and D. Mecerreyes, *Polym. Chem.*, 2013, **4**, 2206–2214.
6 D. Vonlanthen, P. Lazarev, K. A. See, F. Wudl and A. J. Heeger, *Adv. Mater.*, 2014, **26**, 5095–5100.
7 Y. J. Kim, W. Wu, S.-E. Chun, J. F. Whitacre and C. J. Bettinger, *Adv. Mater.*, 2014, **26**, 6572–6579.
8 P. Kumar, E. Di Mauro, S. Zhang, A. Pezzella, F. Soavi, C. Santato and F. Cicoira, *J. Mater. Chem. C*, 2016, **4**, 9516–9525.
9 G. Milczarek, *Electroanalysis*, 2007, **19**, 1411–1414.
10 G. Milczarek and O. Inganäs, *Science*, 2012, **335**, 1468–1471.
11 T. Rębiś, T. Y. Nilsson and O. Inganäs, *J. Mater. Chem. A*, 2016, **4**, 1931–1940.
12 S. Leguizamon, K. P. Díaz-Orellana, J. Velez, M. C. Thies and M. E. Roberts, *J. Mater. Chem. A*, 2015, **3**, 11330–11339.
13 S. Admassie, *Bull. Chem. Soc. Ethiop.*, 2016, **30**, 153–160.
14 S. Admassie, A. Elfwing, E. W. H. Jager, Q. Bao and O. Inganas, *J. Mater. Chem. A*, 2014, **2**, 1974–1979.
15 D. H. Nagaraju, T. Rebis, R. Gabrielsson, A. Elfwing, G. Milczarek and O. Inganäs, *Adv. Energy Mater.*, 2014, **4**, 1–7.
16 S. Admassie, T. Y. Nilsson and O. Inganäs, *Phys. Chem. Chem. Phys.*, 2014, **16**, 24681–24684.
17 S. K. Kim, Y. K. Kim, H. Lee, S. B. Lee and H. S. Park, *ChemSusChem*, 2014, **7**, 1094–1101.
18 G. Milczarek and M. Nowicki, *Mater. Res. Bull.*, 2013, **48**, 4032–4038.
19 F. N. Ajjan, N. Casado, T. Rębiś, A. Elfwing, N. Solin, D. Mecerreyes and O. Inganäs, *J. Mater. Chem. A*, 2016, **4**, 1838–1847.
20 D. C. Marcano, D. V. Kosynkin, J. M. Berlin, A. Sinitskii, Z. Sun, A. Slesarev, L. B. Alemany, W. Lu and J. M. Tour, *ACS Nano*, 2010, **4**, 4806–4814.
21 A. Y. S. Eng, A. Ambrosi, C. K. Chua, F. Šaněk, Z. Sofer and M. Pumera, *Chem.–Eur. J.*, 2013, **19**, 12673–12683.
22 E. Biilmann, *Trans. Faraday Soc.*, 1924, **19**, 676–691.
23 A. M. Navarro-Suárez, J. Carretero-González, V. Roddatis, E. Goikolea, J. Ségalini, E. Redondo, T. Rojo and R. Mysyk, *RSC Adv.*, 2014, **4**, 48336–48343.
24 D. Deng, X. Pan, L. Yu, Y. Cui, Y. Jiang, J. Qi, W. X. Li, Q. Fu, X. Ma, Q. Xue, G. Sun and X. Bao, *Chem. Mater.*, 2011, **23**, 1188–1193.
25 D. Yang, A. Velamakanni, G. Bozoklu, S. Park, M. Stoller, R. D. Piner, S. Stankovich, I. Jung, D. A. Field, C. A. Ventrice and R. S. Ruoff, *Carbon*, 2009, **47**, 145–152.
26 C. Cachet-Vivier, V. Vivier, C. S. Cha, J. Y. Nedelec and L. T. Yu, *Electrochim. Acta*, 2001, **47**, 181–189.
27 Y. Wang, Y. Song and Y. Xia, *Chem. Soc. Rev.*, 2016, **451**, 652–657.
28 H.-J. Shin, S. S. Jeon and S. S. Im, *Synth. Met.*, 2011, **161**, 1284–1288.
29 A. Ganguly, S. Sharma, P. Papakonstantinou and J. Hamilton, *J. Phys. Chem.*, 2011, 17009–17019.
30 Y. J. Oh, J. J. Yoo, Y. Il Kim, J. K. Yoon, H. N. Yoon, J.-H. Kim and S. Bin Park, *Electrochim. Acta*, 2014, **116**, 118–128.
31 V. Khomenko, E. Raymundo-Piñero and F. Béguin, *J. Power Sources*, 2010, **195**, 4234–4241.
32 Y. J. Oh, J. J. Yoo, Y. Il Kim, J. K. Yoon, H. N. Yoon, J. H. Kim and S. Bin Park, *Electrochim. Acta*, 2014, **116**, 118–128.